



ISME

# Modeling and Wrench Feasible Workspace Analysis of a Cable Suspended Robot for Heavy Loads Handling

**J. Hamedi**<sup>1</sup>  
Associate Professor

**H. Zohoor**<sup>2</sup>  
Graduate student

*Modeling and Wrench feasible workspace analysis of a spatial cable suspended robots is presented. A six-cable spatial cable robot is used the same as Stewart robots. Due to slow motion of the robot we suppose the motion as pseudostatic and kinetostatic modeling is performed. Various workspaces are defined and the results of simulation are presented on the basis of various workspaces and applied wrenches (forces/moments) on the robot. The results show that enlarging the size of fixed platform, increasing vertical payload, reducing applied lateral forces and elimination of applied moments on moving platform, cause expansion of workspaces volumes for the purpose of heavy loads handling.*

*Keyword:* cable suspended robot, wrench, workspace, modeling, heavy loads handling

## 1. Introduction

Cable suspended robots support a moving platform (MP) in space by several spatially arranged cables with computer-controlled winches. The winches are mounted on base platform (BP). Compared to conventional robots, it is possible to control not only the translational motion of the payload but also its orientation in order to perform, for example, loads handling. By this, cable suspended robots combine the ability of cranes to support heavy payloads in a large workspace with the dexterity of robot manipulators. MP may be equipped with various attachments, including hooks, cameras, electromagnets and robotic grippers. One significant difference between cable suspended robots and classic Stewart robots is that cables only apply tensile force in MP. However, the advantages of this type of actuation are numerous and incontestable. Firstly, cables allow incomparable motion range that is much larger than that of conventional actuators, such as hydraulic cylinders, and take up only a little space when rolled around a spool. Secondly, as the cables are being used only in tension, they are, for a similar task, much thinner and lighter than most conventional mechanical components. Thus, they have negligible inertia and are particularly suitable for systems in which great accelerations are applied. Furthermore, cables are less expensive than hydraulic cylinders and, being much more flexible, they provide a kind of natural protection in the case of interference. Consequently, cable robots are exceptionally well suited for many

<sup>1</sup>Corresponding Author, Phd student, Department of Mechanical Engineering, Science and Research Branch, Islamic Azad University, Tehran, Iran

<sup>2</sup>Distinguished Professor and Member, Center of Excellence in Design, Robotics and Automation, School of Mechanical Engineering, Sharif University of Technology, Tehran, Iran; Fellow, The Academy of Sciences of IR Iran

applications such as material handling, manipulation of heavy payloads, rescue robots and cleanup of disaster sites. On the other hand, cable robots do sacrifice some accuracy due to cable sag and stretch. Applications are, for example, precise handling and assembling large and heavy components on construction. Cable suspended robots were studied first in U.S. in 1989[1]. Cable robots static is different from Stewart platform statics due to cables individual property but their kinetic is slightly similar to Stewart platform [2]. Many studies have been conducted on statics and kinetics of Stewart platform and some on statics and kinematics of cable system [3]. Georgia Institute of Technology [4] and Ohio University [5] have recently focused one of their important studies on cable suspended robots. Many research have been conducted on planar cable robots[6,7]. Furthermore, some research have been conducted on their application in manufacturing in large scale, heavy industries[8], spatial industries[9], wind tunnel [10] and construction cranes[11]. The Robocrane is a cable driven, multi-purpose manipulator based on the Stewart Platform Parallel link manipulator. It consists of 6 cables spanned in the same manner as a Stewart platform type parallel mechanism [12]. In this robot, since gravity force plays a roll of a cable tension, six is enough for satisfying the condition of cable tension. This mechanism is suitable for the accurate positioning of heavy objects. The workspace of cable suspended robot is different from Stewart platform. Stewart platform workspace depends on its geometry [13]. Some research have been conducted on dynamic workspace [14]. These robots are in different types that it is impossible to study and survey all of them but what is focused in this research is studying type of them used for handling loads, moving them through a specific path and unloading them. In these robots which are used mainly in heavy industries, the load is tolerated by cables. This paper attempts to tackle some aspects of workspace analysis of a 6DOF cable robot by addressing the variations of the workspace volume and the accuracy of the robot using different parameters. The structure of the paper is as follows: Second section has been dedicated to kinetostatic modeling. Discussion about kinematic subjects is conducted, and kinematic modeling is performed by selecting a suitable structure and kinematic equations of the system are detected. Considering robot slow motion, we consider the motion as pseudostatic motion and static equilibrium equations are derived. In the third section, analysis of cable robots is performed by workspace definition and its analysis. Various workspaces of these robots are defined and workspace volume is gained for various Stewart cable robots. Analysis of various workspaces is performed by changing different parameters. Since the cable forces should always be tensional, this condition is always considered in the analysis of workspace. The forth part is dedicated to conclusion. Achieved results are presented in this part.

## **2. Kinetostatic Modeling**

### *2.1. Geometrical Modeling*

Cable robots classification was first conducted in 1994[15]. In one of these types, the number of cables ( $m$ ) is less than or equal to the number of degrees of freedom ( $n$ ). These robots are called Incompletely Restrained Positioning Mechanism (IRPM). They also can have less than  $n$  cables and thus the pose (position and/or orientation) of MP is not completely determined by the lengths of the cables. Instead, these manipulators rely on the presence of gravity to determine the resulting pose of MP and they are exceptionally well suited for manipulation of heavy payloads. Because the concentration of this research is on applying these robots for heavy loads handling, the IRPM robot is chosen and regarding to tendency to creating six-degree of freedom on motion, we consider six cable model[16]. Structure is considered in accordance to Figure 1. Basic points  $C_1, \dots, C_6$  all locate in the same plane with  $Z$  coordinate. These points locate in the same radial distance from  $XYZ$  coordinate system that locates in the center of BP. MP also has a set of connection points  $D_1, \dots, D_6$  that locates in the same

radial distance from  $O_M$  the center of mass of the MP.  $r_{base}$  is the radial distance from  $O_F$  the coordinate system origin of XYZ frame. We can define the position vectors of connection points in moving platform relative to  $O_M$  the coordinate system origin.  $r_{end}$  is the radial distance from the coordinate system origin of XYZ base.  $\gamma$  is the angle between BP connection points meaning  $(C_1,C_2),(C_3,C_4),(C_5,C_6)$  and MP connection points meaning  $(D_1,D_6), (D_2,D_3), (D_4,D_5)$  [16]. Structures for  $\gamma=0^\circ$  and  $\gamma=45^\circ$  are equilateral triangles and symmetric hexagons respectively, similar to Stewart platform 6-6 shown in Figure 2.

## 2.2. Kinematics equations

Position vector from  $C_i$  to  $D_i$  or cable length vector shown in Figure 3, can be written relative to basic coordinates frame:

$$\vec{l}_i = \vec{r} + [R]^M \vec{d}_i - \vec{c}_i \quad i = 1, \dots, 6 \quad (1)$$

where:

$\mathbf{c}_i$ : Position vector of point  $C_i$  as  $C_i(X_{C_i}, Y_{C_i}, Z_{C_i})$

$\mathbf{d}_i$ : Position vector of point  $D_i$  as  $D_i(X_{D_i}, Y_{D_i}, Z_{D_i})$

$r$ : Position vector of point  $O_M$  center of moving platform (X,Y and Z components in fixed frame)

$l_i$ : Distance between  $C_i$  and  $D_i$  ( $i$ th cable length)

If  $R$  shows rotation matrix of the moving platform with respect to base platform with rotation angles  $\psi, \theta, \phi$  about fixed axes:

$$\begin{bmatrix} X \\ Y \\ Z \end{bmatrix} = R(\psi, \theta, \phi) \begin{bmatrix} x \\ y \\ z \end{bmatrix} \quad (2)$$

where:

$$R = \begin{bmatrix} C\phi C\theta & -S\phi C\psi + C\phi S\theta S\psi & S\phi S\psi + C\phi S\theta C\psi \\ S\phi C\theta & C\phi C\psi + S\phi S\theta S\psi & -C\phi S\psi + S\phi S\theta C\psi \\ -S\theta & C\theta S\psi & C\theta C\psi \end{bmatrix} \quad (3)$$

cable length vector is defined by :

$$\vec{l} = [l_1 \ l_2 \ \dots \ l_m] \quad (4)$$

the length of cables is:

$$l_i^2 = \|\vec{l}_i\|^2 = \vec{l}_i^T \vec{l}_i \quad (5)$$

the posture (position and orientation) vector of MP is as follow:

$$\mathbf{u} = [x \ y \ z \ \psi \ \theta \ \phi]^T \quad (6)$$

## 2.3. Kinetics equations

Considering focused usage of these robots on handling heavy loads, robot speed considered minor and its motion assumed as pseudostatic motion. In this state, survey and kinetic

modeling will be converted to static modeling. Cable robots move using servo motors that control in cable tensions. Because all cables are connected to MB, forces in end MB are directly related to tension quantity and direction. For finding forces at MB by tension mean, virtual task principle is applied. Cable suspended robot moves by servomotor that controls tension in cables. Since the cables are joined to MB, forces in MB are directly in relation to tension magnitudes and their directions. In order to find forces in MB using tension magnitude, the virtual work principle is applied. Suppose  $\mathbf{f}_{ext}=[f_x \ f_y \ f_z \ m_x \ m_y \ m_z]^T$  displays output wrench vector in MB and  $\mathbf{s}=[s_1 \ s_2 \ s_3 \ s_4 \ s_5 \ s_6]$  displays applied-by-servomotors tensions vector, in cables. In this condition, if  $\delta\mathbf{u}=[\delta x \ \delta y \ \delta z \ \delta\psi \ \delta\theta \ \delta\phi]$  displays virtual displacements vector in MB produced by  $\mathbf{f}_{ext}$ , and  $\delta\mathbf{q}=[\delta q_1 \ \delta q_2 \ \delta q_3 \ \delta q_4 \ \delta q_5 \ \delta q_6]$  displays virtual displacements vector in cables produced by  $\mathbf{s}$ , according to virtual work principle for MP:

$$\delta W = \mathbf{s}^T \delta \mathbf{q} - \mathbf{f}_{ext}^T \delta \mathbf{u} = 0 \quad (7)$$

The reason for the negative sign for the  $\mathbf{f}_{ext}^T \delta \mathbf{u}$  term is due to the definition of  $\mathbf{f}_{ext}$  is the forces vector and external torques for MP. Positive sign in front of the term  $\mathbf{s}^T \delta \mathbf{q}$  is due to similarity in direction tension and displacement of the cables.

Jacobian matrix is the matrix which transports the velocity of MP to the velocity of cables:

$$J_{ij} = \frac{\partial q_i}{\partial u_j} \quad (8)$$

then

$$\delta \mathbf{q} = \mathbf{J} \delta \mathbf{u} \quad (9)$$

substituting (9) in (7):

$$(\mathbf{s}^T \mathbf{J} - \mathbf{f}_{ext}^T) \delta \mathbf{u} = 0 \quad (10)$$

and

$$\mathbf{s}^T \mathbf{J} - \mathbf{f}_{ext}^T = 0 \quad (11)$$

finally after simplicity:

$$\mathbf{J}^T \mathbf{s} = \mathbf{f}_{ext} \quad (12)$$

The matrix  $\mathbf{J}^T$  is posture-dependent matrix:

$$\mathbf{J}^T = \begin{bmatrix} \left( \frac{\vec{l}_1}{|l_1|} \right)^T & \left( {}^{o_f} \vec{d}_1 \times \frac{\vec{l}_1}{|l_1|} \right)^T \\ \vdots & \dots \\ \left( \frac{\vec{l}_m}{|l_m|} \right)^T & \left( {}^{o_f} \vec{d}_m \times \frac{\vec{l}_m}{|l_m|} \right)^T \end{bmatrix} \quad (13)$$

The matrix is called structure matrix and its dimension is  $n \times m$ .

### 3. Modeling based on workspace

In order to simulate the robot on the basis of workspace, we should first define workspace according to its categorizations.

#### 3.1. Types of workspace

The workspace of a robotic system is defined as the volume that the reference point of MP can reach. In cable suspended robots, the kinds of workspace are defined. Reachable Workspace Volume (RWV) is defined as the volume that can be reached by the reference point regardless of the MP orientation. The Statically Reachable Workspace Volume (SRWV) is the volume that MP must be in equilibrium because of the fact that cables cannot sustain compressive forces and all cable tensions must be non-negative to equilibrate the MP for an applied force. Constant Orientation Workspace Volume (COWV) can be determined as set of locations of reference point  $O_M$  that can be reached with some orientations within a set of defined ranges on the orientation parameters. Total Orientation Workspace Volume (TOWV) is the same as the COWV but point  $O_M$  can be reached with all orientations. Wrench feasible Workspace Volume (WFVV) is the volume that considering effects of external factors caused by applied external forces and torques to MP, all cables are in tension for static equilibrium of MP.

#### 3.2. Simulation Algorithm

Considering kinetostatic modeling and the kinds of workspace, the programs have been written using Matlab which analyze SCWV. The external applied wrench is the weight of load that is lifted by robot. By selecting the search space as a cube with BP dimensions and the range of cable length, the tension of cable is calculated:

$$\left\{ \begin{array}{l} \text{under} \\ \left\{ \begin{array}{l} s = J^{-T} f_{ext} \\ s \in [s_{min}, s_{max}] \\ s_i \geq 0 \therefore i = 1, \dots, 6 \end{array} \right. \end{array} \right. \quad \text{and} \quad l_{min} \leq l_i \leq l_{max} \quad (14)$$

Solving Eq. (14) is depended to full ranking of structure matrix. Cables length limitation will be specified based on workspace volume. Minimum tension of cables is determined for preventing from cables slack and their maximum is determined by the actuators tensional forces. While selecting a point in workspace volume, equations and constraint are satisfied, the point is considered as the one in workspace, otherwise that point doesn't belong to workspace. Then the next point will be checked and the operation will be repeated till last point of research workspace. Number of all obtained points by this system, is called workspace volume. Simulation algorithm is shown in Figure 4.

The assumptions used in this research are:

- searching volume  $-8 \leq X \leq 8$ ,  $-8 \leq Y \leq 8$ ,  $0 \leq Z \leq 10$  m
- The size of searching step in direction of the three axes  $\Delta X = \Delta Y = \Delta Z = 0.4$  m
- The minimum of cables length  $l_{min} = 0$  and the maximum cables length  $l_{max} = 15$  m
- The minimum cables tension is  $s_{min} = 5$  kN and the maximum of cables tension is  $s_{max} = 55$  kN
- The geometric configuration of platforms is  $\gamma = 0^\circ, 15^\circ, 30^\circ$  and  $45^\circ$ .
- External applied wrench  $f_{ext} = [0 \ 0 \ 100 \ 0 \ 0 \ 0]^T$  kN

Now by using the shown algorithm in figure 4 and considered assumptions, simulation will be done for kinds of defined workspace

### 3.2.1. SRWV

We obtain SRWV for two different geometric configuration  $\gamma = 0$  and  $\gamma = 45$  and for all of the MP orientation. Figures 5 and 6 show SRWV as form of a complete volume of three dimensional mesh with a triangular base and regular hexagon in which for  $\gamma = 0$  and  $\gamma = 45$ , these are 8217 and 9389 points, respectively.

### 3.2.2. COWV

MP rotation is constant here. Among numerous constant MP rotation angles, zero degree angles are selected and workspace are calculated and drawn. Figures 7 to 10 in sequence show SCWV for four different geometrical configuration of  $\gamma = 45^\circ$ ,  $\gamma = 30^\circ$ ,  $\gamma = 15^\circ$  and  $\gamma = 0^\circ$ . Number of resulted points for these four configuration in sequence are 375 points for  $\gamma = 45^\circ$ , 1375 points for  $\gamma = 30^\circ$ , 2500 points for  $\gamma = 15^\circ$  and 3675 points for  $\gamma = 0^\circ$ . Workspace volume decrease apparently toward SRWV. Figure 11 show the effect of geometrical shape on COWV. It is observed that when platform geometrical shape changes from regular hexagonal to triangular configuration, the workspace volume increases. Figure 12 shows the effects of BP size and geometrical configuration on COWV. It is perceived that when the geometrical shape of platform changes to triangular configuration and size of BP become larger simultaneously, workspace volume will be increased.

### 3.2.3. TOWV

Considering large number of MP rotating angles, these kinds of workspace will be obtained hardly. We select two configuration of  $\gamma = 0$  and  $\gamma = 45$  for MP rotation angles in the range  $30^\circ \leq \psi \leq 30^\circ$ ,  $-10^\circ \leq \theta \leq 10^\circ$ ,  $-5^\circ \leq \phi \leq 5^\circ$  and the search is calculated among the volume of 4000 points. Figures 13 and 14 show TOWV with 561 and 12 points for geometrical configuration of  $\gamma = 0$  and  $\gamma = 45$ , respectively.

Figure 15 illustrates the changing size of different workspaces as SRW, COWV and TOWV for different configurations of BP and MP. Obviously the size of workspace for TOWV will be decreased, and configuration  $\gamma = 0$  has a larger size of workspace than configuration of  $\gamma = 45$ .

### 3.2.4. WFWV

Applied External wrench to MP is column vector with six components (three forces and three torques around three axes with coordinate center on mass center of MP). In the previous section, the only considered applied force to MP in line with z axis. But here, we are studying the effects of changes in applied forces and torques to MP in workspace. As mentioned before, this type of workspace is called wrench feasible workspace volume (WFWV).

$$\mathbf{f}_{\text{ext}} = [f_x \quad f_y \quad f_z \quad m_x \quad m_y \quad m_z]^T \quad (15)$$

Figures 15 to 22 illustrate applied external wrench changes and  $\gamma$  in WFW for MP constant rotation and  $\psi = 0^\circ$ ,  $\theta = 0^\circ$  and  $r_{\text{end}}/r_{\text{base}} = 1$ . In all forms, four curves from top to bottom that are in sequence include  $\gamma = 0, 15, 30$  and  $45$ . Assuming  $f_x = 100$  KN Figures 16 and 17 show effects of change in  $f_y$ ,  $f_z$  and  $\gamma$  in WFW for  $r_{\text{base}} = 6\text{m}$  and  $r_{\text{base}} = 12\text{m}$  in sequence. For  $f_z = 100$  KN Figures 18 and 19 show effects of change in  $f_x$ ,  $f_y$  and  $\gamma$  in WFW for  $r_{\text{base}} = 6\text{m}$  and  $r_{\text{base}} = 12\text{m}$  in sequence. Assuming  $m_x = 100$  KNm Figures 20 and 21 illustrate change effects of  $m_y$ ,  $m_z$  and  $\gamma$  in WFW for  $r_{\text{base}} = 6\text{m}$  and  $r_{\text{base}} = 12\text{m}$  in sequence. For  $m_z = 100$  kNm Figures 22 and 23 illustrate effects of change in  $m_x$ ,  $m_y$  and  $\gamma$  in WFW for  $r_{\text{base}} = 6\text{m}$  and  $r_{\text{base}} = 12\text{m}$  in sequence. Because of platform symmetry only one of  $f_x$  and  $f_y$  changes were studied.

#### 4. Conclusion

For handling heavy loads in large workspace a spatial cable robot with six degree of freedom and six cables could be used as IRPM. RWV is larger than the other workspaces, but it is not useable workspace in handling heavy loads. SRWV under vertical force of weight and for the whole orientation of triangular configuration is less than hexagon configuration. The geometric shape of platforms affects on COWV as it increases when BP enhances and  $\gamma$  reduces. TOWV in compare to COWV reduces significantly. When size of BP grows up, SCWV increase and it will hold true for all orientation. That means with making BP larger, SCWV enhances. Reducing the lateral forces  $f_x$  and  $f_y$ , elimination the applied torques and increasing the vertical force  $f_z$  and size of BP will lead to the increasing of WFWV.

#### References

- [1] Nicholas, G. , “Stiffness Study of a Parallel Link Robot Crane for Shipbuilding Applications,” *ASME Journal of Offshore Mechanics and Arctic Engineering*, Vol.111, pp.183-193 (1989).
- [2] Alan, M., “Development of a Robotic Structural Steel Placement System,” Report Official Contribution of the National Institute of Standards and Technology ,NIST (2003).
- [3] Roberts, R. G., Graham, T., and Lippitt, T., “On the Inverse Kinematics, Statics , and Fault Tolerance of Cable-Suspended Robots,” *Journal of Robotic Systems*, Vol. 15, pp.581-597 (1998).
- [4] Ebert-Uphoff, I. , “What A Stability Measure for Underconstrained Cable-Driven Robots,” *Proceedings of the 2004 IEEE International Conference on Robotics & Automation* , pp.4943-4949 ( 2004).
- [5] Vadia, J. , “Planar Cable Direct Driven Robot : Hardware Implementation , ” MSc. Thesis, Department of Mechanical Engineering, Ohio (2003).
- [6] Robert L., and Williams II, “Planar Cable-Direct- Driven Robots, Part I : Kinematics and Statics ,” *ASME Design Automation Conference*, pp.1-9 (2001).
- [7] Williams II, R., and Gallina , P., “Planar Cable-Direct-Driven Robots :design for wrench exertion, ” *Journal of Intelligent and Robotic Systems*, Vol.35, pp. 203-219 (2002).
- [8] Albus, S., Dagalakis, G., and Yancey, W., “Available Robotics Technology for Applications in Heavy Industry,” *Iron and Steel Exposition and Annual Convention*, pp.117-115 (1988).
- [9] Kossowski, C., and Notash, L., “A Novel 4 DOF Cable Actuated Parallel Manipulator,” *J. Robotic Systems*, Vol.19, pp.605-615 (2002).
- [10] Shiang, W. J., Cannon, D., and Gorman, J., “Dynamic Analysis of the Cable Array Robotic Crane,” *Proceeding of IEEE Conference on Robotics and Automation*, pp.2495-2500 (1999).

- [11] Shiang, W. J., Cannon, D., and Gorman, J., “Dynamic Analysis of the Cable Array Robotic Crane,” *Proceeding of 1998 IEEE Conference on Robotics and Automation*, pp. 2495-2500 (1999).
- [12] Do, W. Q., and Yang, D.C. H., “Inverse Dynamic Analysis and Simulation of a Platform Type of Robot,” *Journal of Robotic Systems*, Vol. 5, pp.209-222 (1988).
- [13] Agrawal, S. K., “Workspace Boundaries of In-Parallel Manipulator Systems,” *International Journal of Robotics and Automation*, Vol. 7, pp.94-99 (1998).
- [14] Sunil K. , “Cable Suspended Planar Robots With Redundant Cables: Controllers With Positive Tensions,” *IEEE Transactions on Robotics*, Vol. 21, pp.143-150 ( 2005).
- [15] Verhoeven, R., Hiller, M., and Tadokoro, S., “Workspace, Stiffness, Singularities and Classification of Tendon-Driven Stewart Platforms,” *6th International Symposium on Robot Kinematics*, pp.105-114(1998).
- [16] Pusey, J., Fattah, A., and Agrawal, S. , “Design and Workspace Analysis of a 6-6 Cable Suspended Parallel Robot, ” *Mechanism and Machine Theory* , Vol.39, pp.761–778 (2004).

## Nomenclature

$C_i$	corner points of the base platform
$c_i$	Position vector of point $C_i$
$D_i$	corner points of the moving platform
$d_i$	Position vector of point $D_i$
$f_{ext}$	vector of external forces and torques applied to the moving platform
$f_x, f_y, f_z$	applied forces to the moving platform in directions x,y and z axes respectively
$i$	cable number
$J$	Inverse Jacobian
$J^T$	structure matrix
$l_i$	distance between $C_i$ and $D_i$ ( $i_{th}$ cable length)
$l_{min}$	minimum length of cables
$l_{max}$	maximum length of cables
$m_x, m_y, m_z$	applied moments to the moving platform about three axes x, y and z respectively.
$O_F$	center of the fixed inertia coordinate XYZ ( surface center of base platform)
$O_M$	center of principal body coordinate xyz ( center of mass of moving platform)
$\delta q$	MP velocity in the inertial coordinates
$r$	Position vector of $O_M$
$r_{base}$	radius of points of connections of the cables to the base platform from $O_F$
$r_{end}$	radius of points of connections of the cables to the moving platform from $O_M$
$R$	rotation matrix of the moving platform with respect to the base platform
$s$	vector of applied tensions by servo-motors in the cables
$s_{min}$	minimum tension in the cables
$s_{max}$	maximum tension in the cables
$u$	posture of the moving platform
$\delta u$	joint rates of the actuator
$x,y,z$	principal body coordinate of the center of mass of the moving platform
$X,Y,Z$	fixed inertia coordinate of the surface center of the base platform

$\Delta X, \Delta Y, \Delta Z$	magnitude of search step in directions of all three axes
MP	Moving platform
BP	Base platform
IRPM	Incompletely Restrained Positioning Mechanism
RWV	Reachable Workspace Volume
SRWV	Statically Reachable Workspace Volume
SCWV	Statically Combined Workspace Volume
COWV	Combined Workspace Volume
TOWV	Total Orientation Workspace Volume
WFWV	Wrench Feasible Workspace Volume

*Greek symbols*

$\psi$	angle of rotation of the moving platform about the fixed axis of X
$\theta$	angle of rotation of the moving platform about the fixed axis of Y
$\varphi$	angle of rotation of the moving platform about the fixed axis of Z
$\gamma$	angle between BP connection points and MP connection points

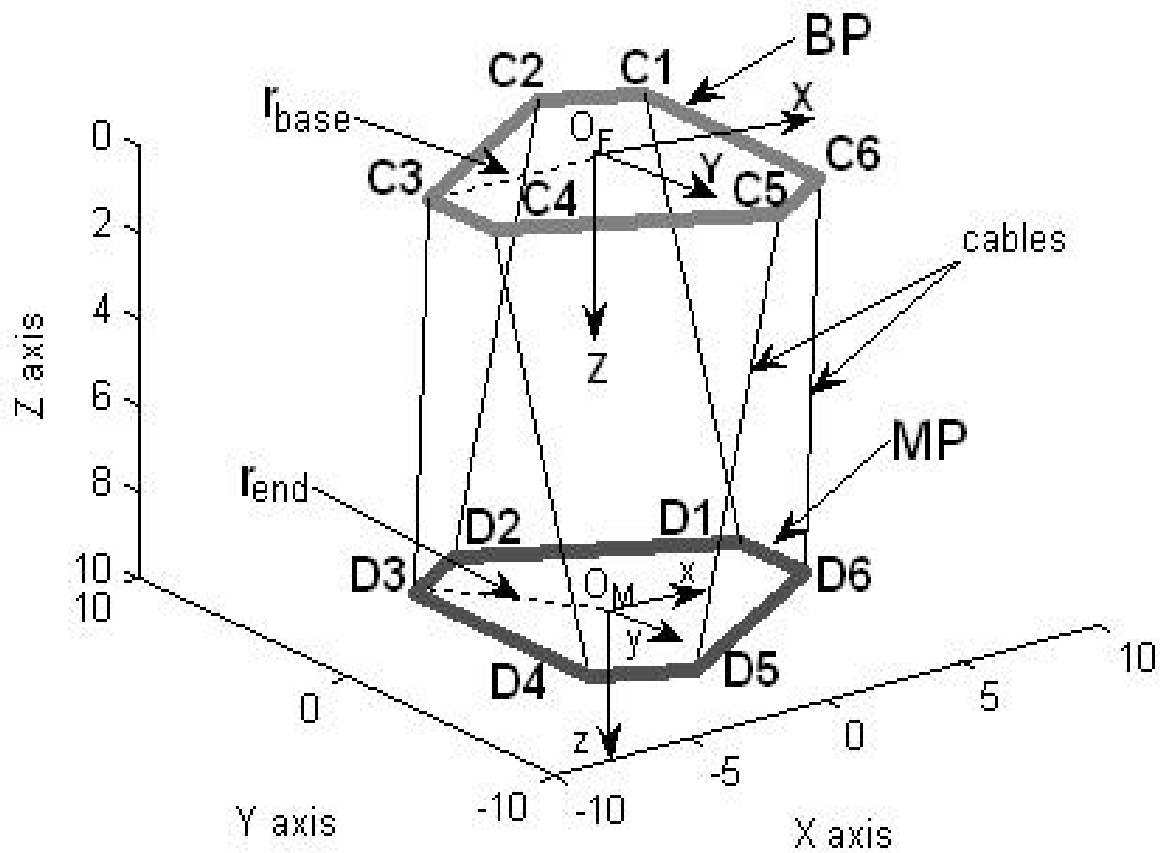


**Figure1** under study model

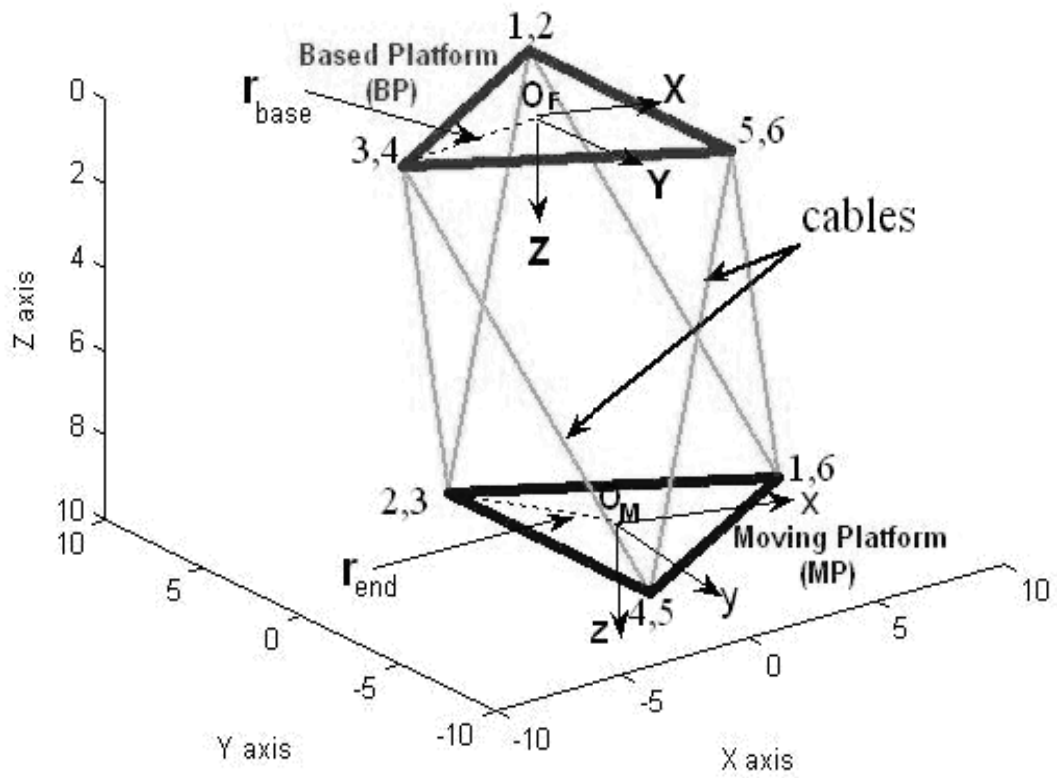


**Figure 2** the schematic of moving platform with the configuration of  $\gamma = 0$

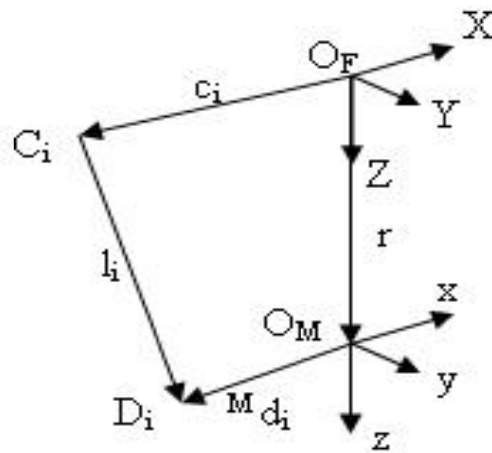


**Figure 3**  $i^{\text{th}}$  cable vector polygon.

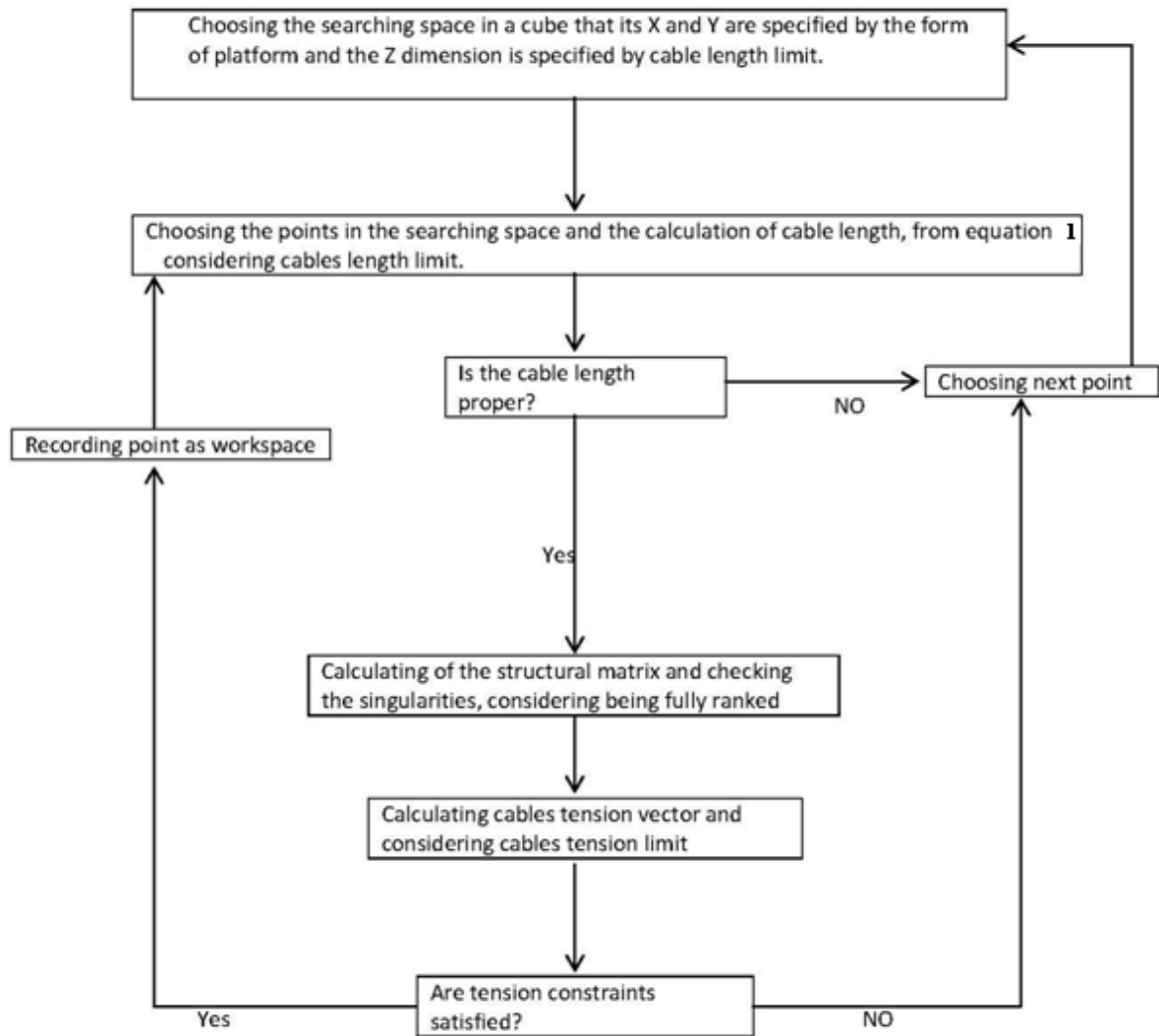
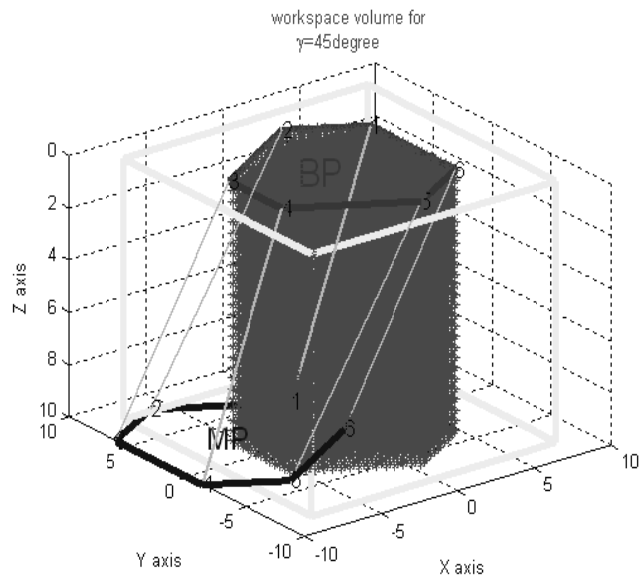
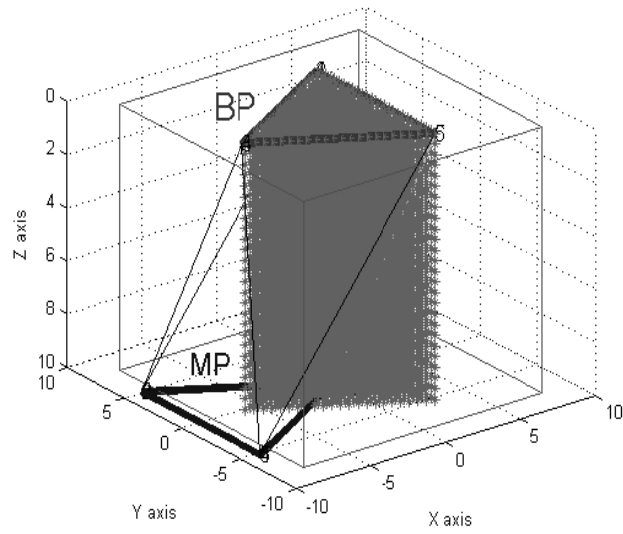


Figure 4 Simulation Algorithm



**Figure 5** SRW for  $\gamma = 0$



**Figure 6** SRW for  $\gamma = 45^\circ$

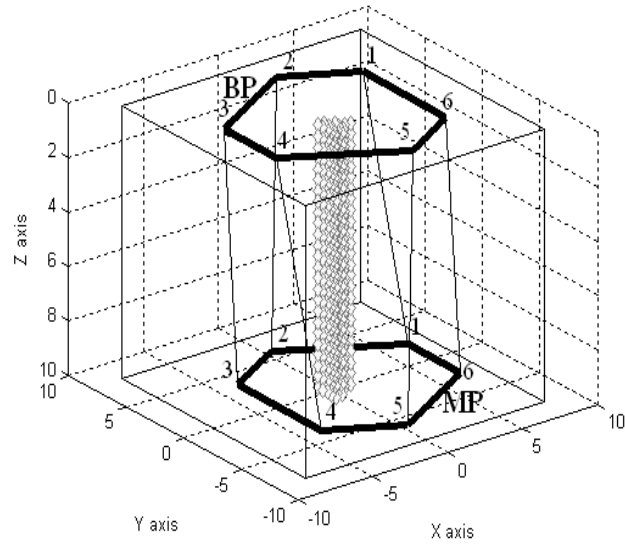


**Figure 7** COWV for  $\gamma=45^\circ, \psi=0^\circ, \theta=0^\circ$  and  $\varphi=0^\circ$

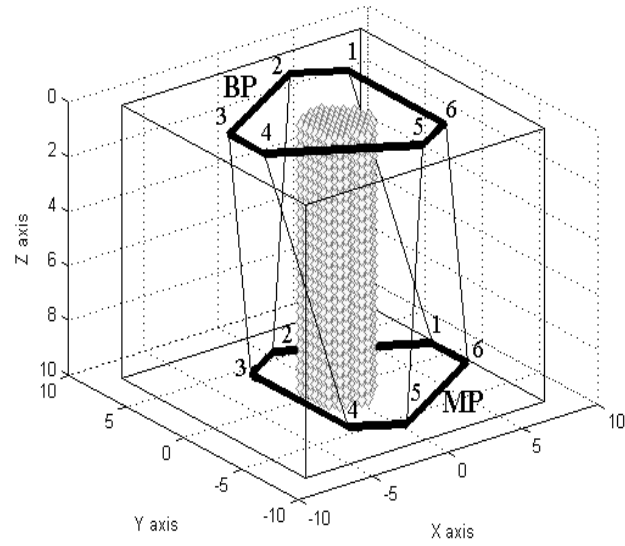


**Figure 8** COW for  $\gamma=30^\circ, \psi=0^\circ, \theta=0^\circ$  and  $\varphi=0^\circ$

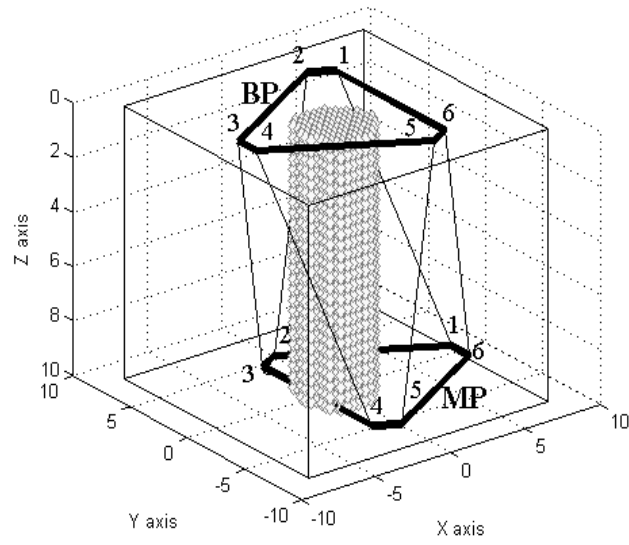


**Figure 9** COWV for  $\gamma=15^\circ, \psi=0^\circ, \theta=0^\circ$  and  $\varphi=0^\circ$

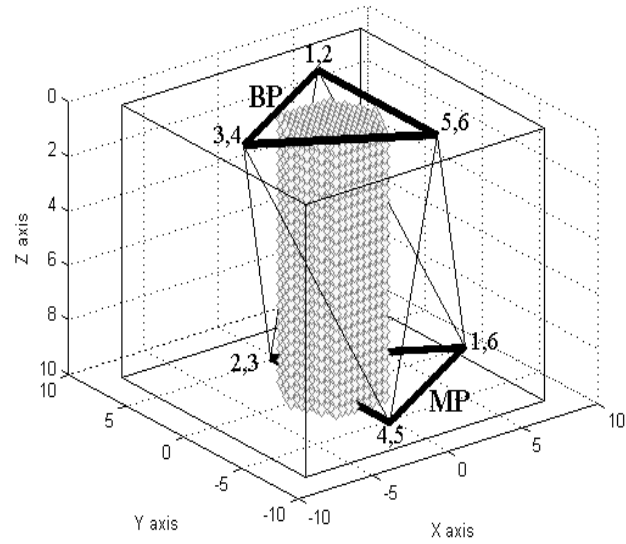


**Figure 10** COWV for  $\gamma=0^\circ, \psi=0^\circ, \theta=0^\circ$  and  $\varphi=0^\circ$

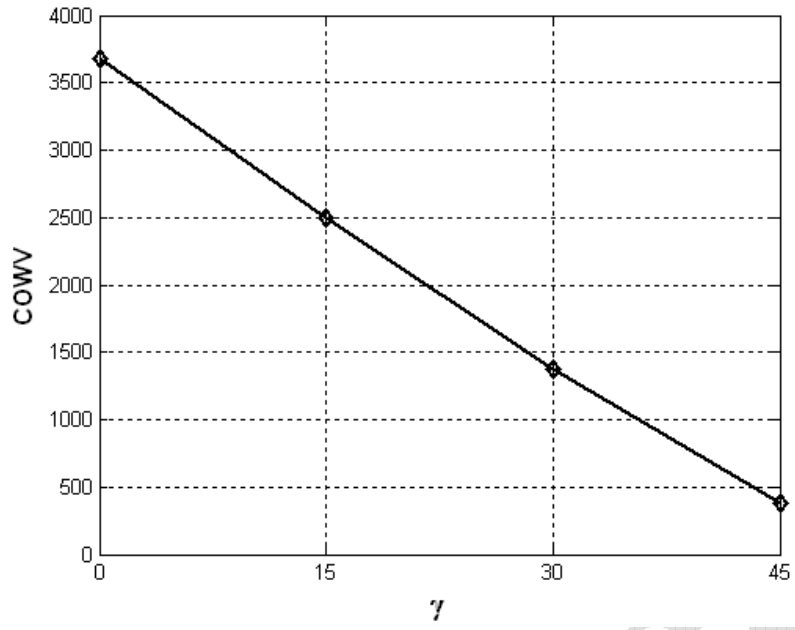


Figure 11 the effect of geometrical shape on COWV

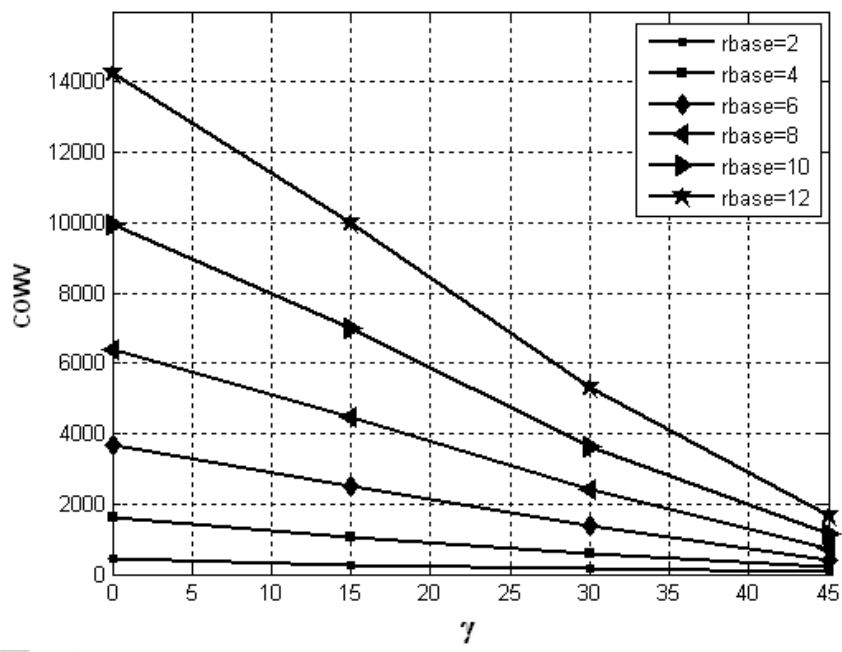
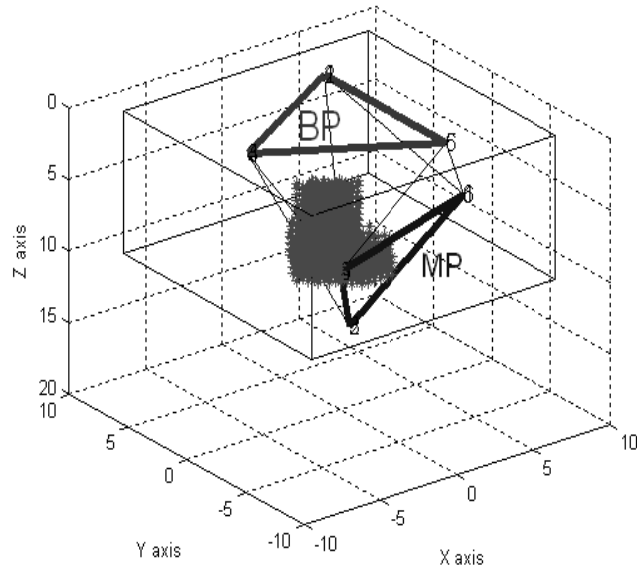
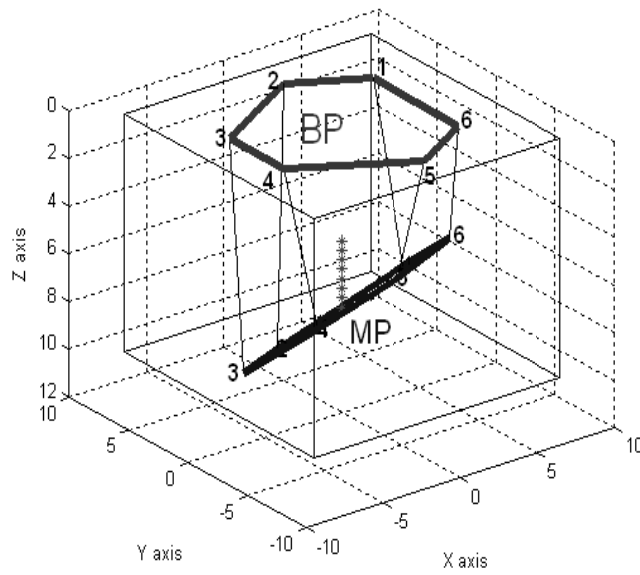


Figure 12 the effect of BP measurement and geometrical shape on COWV



**Figure 13** TOWV for  $\gamma = 0^\circ$



**Figure 14** TOWV for  $\gamma = 45^\circ$

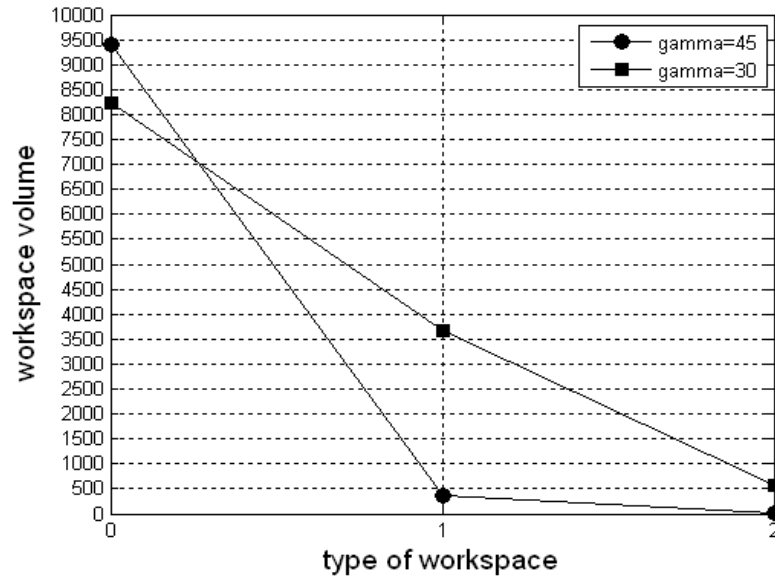


Figure 15 variation of workspace volumes for  $\gamma = 0^\circ$  and  $\gamma = 45^\circ$  0:SRWV 1:COWV 2:TOWV

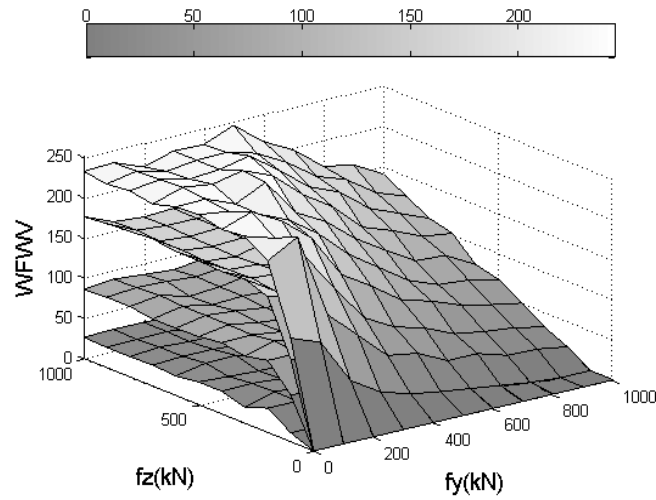


Figure 16 variation of  $f_y$ ,  $f_z$  and  $\gamma$  on WFWV ( $r_{base}=6m$ )

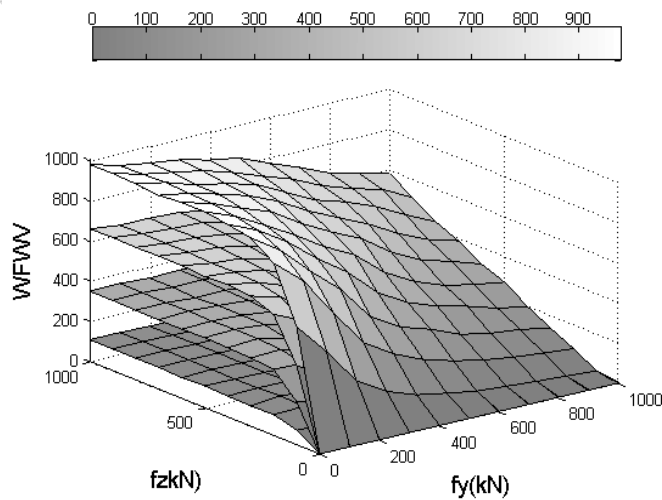
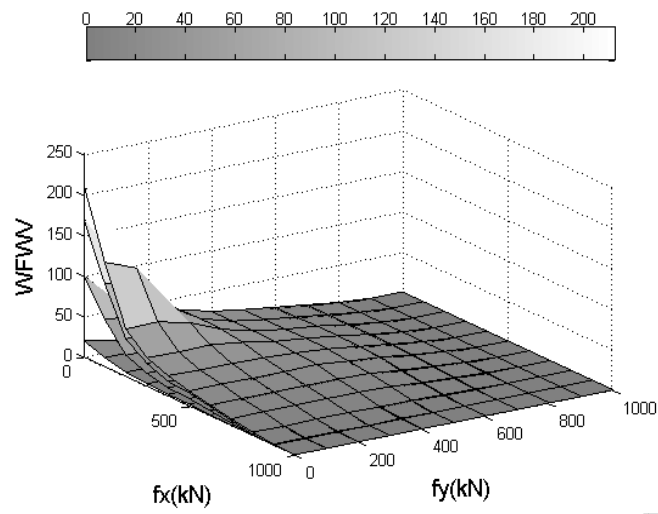
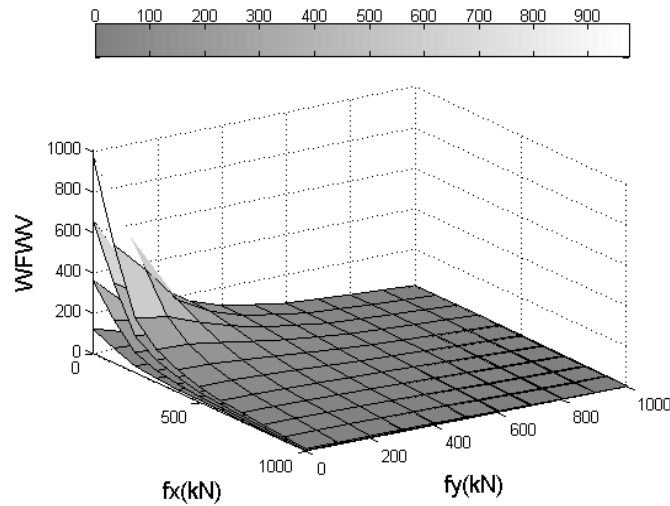


Figure 17 variation of  $f_y$ ,  $f_z$  and  $\gamma$  on WFWV ( $r_{base}=12m$ )



**Figure 18** variation of  $f_x$ ,  $f_y$  and  $\gamma$  on WFWV ( $r_{base}=6m$ )



**Figure 19** variation of  $f_x$ ,  $f_y$  and  $\gamma$  on WFWV ( $r_{base}=12m$ )

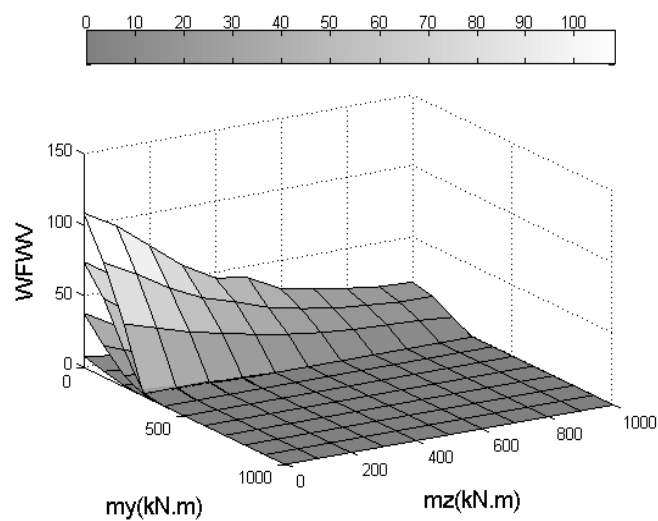


**Figure 20** variation of  $m_y$ ,  $m_z$  and  $\gamma$  on WFWV ( $r_{base}=6m$ )

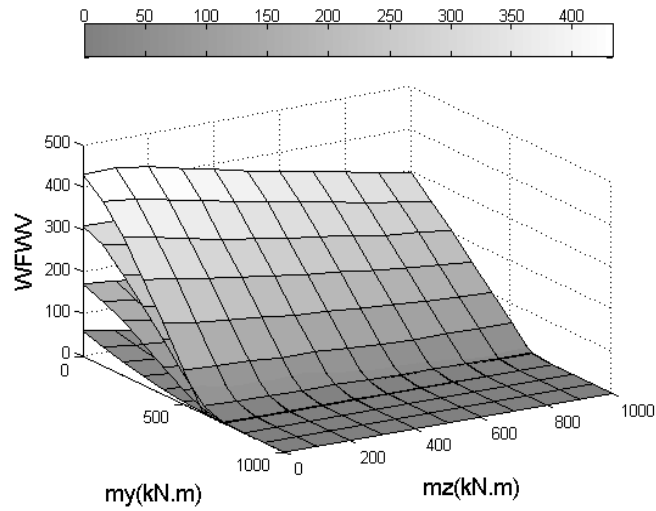


Figure 21 variation of  $m_y$ ,  $m_z$  and  $\gamma$  on WFWV ( $r_{base}=12m$ )

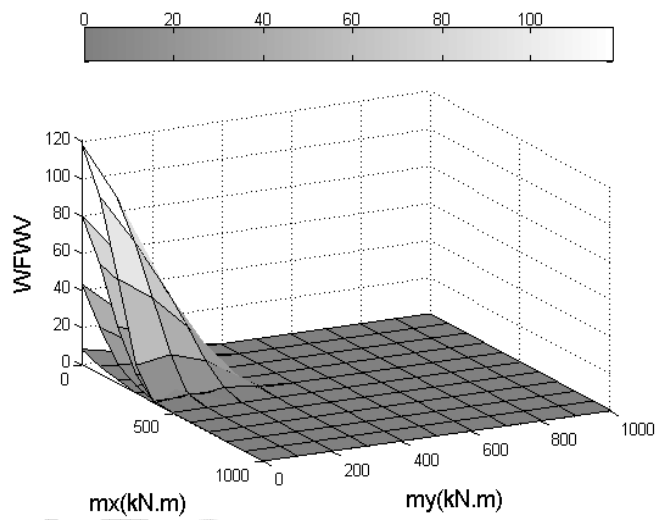


Figure 22 variation of  $m_x$ ,  $m_y$  and  $\gamma$  on WFWV ( $r_{base}=6m$ )

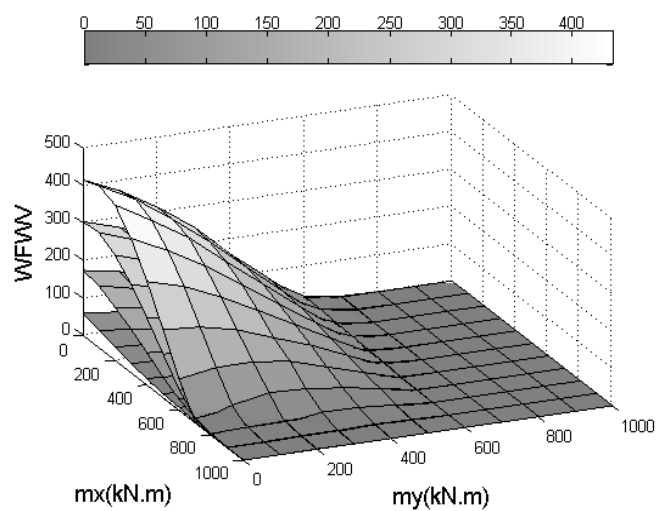


Figure 23 variation of  $m_x$ ,  $m_y$  and  $\gamma$  on WFWV ( $r_{base}=12m$ )

